Atmos. Chem. Phys. Discuss., 9, 13629–13653, 2009
www.atmos-chem-phys-discuss.net/9/13629/2009/

Atmospheric Chemistry and Physics Discussions

This discussion paper is/has been under review for the journal *Atmospheric Chemistry and Physics (ACP)*. Please refer to the corresponding final paper in *ACP* if available.

Rapid formation of isoprene photo-oxidation products observed in Amazonia

T. Karl[1], **A. Guenther**[1], **A. Turnipseed**[1], **P. Artaxo**[2], **and S. Martin**[3]

[1]National Center for Atmospheric Research, 1850 Table Mesa Dr, Boulder, 80301, CO, USA
[2]Instituto de Fisica, Universidade de Sao Paulo, Sao Paulo, Brazil
[3]School of Engineering and Applied Sciences & Department of Earth and Planetary Sciences, Harvard University, Cambridge, MA, USA

Received: 20 May 2009 – Accepted: 9 June 2009 – Published: 22 June 2009

Correspondence to: T. Karl (tomkarl@ucar.edu)

Published by Copernicus Publications on behalf of the European Geosciences Union.

Abstract

Isoprene represents the single most important reactive hydrocarbon for atmospheric chemistry in the tropical atmosphere. It plays a central role in global and regional atmospheric chemistry and possible climate feedbacks. Photo-oxidation of primary hydrocarbons (e.g. isoprene) leads to the formation of oxygenated VOCs (OVOCs). The evolution of these intermediates affects the oxidative capacity of the atmosphere (by reacting with OH) and can contribute to secondary aerosol formation, a poorly understood process. An accurate and quantitative understanding of VOC oxidation processes is needed for model simulations of regional air quality and global climate. Based on field measurements conducted during the Amazonian aerosol characterization experiment (AMAZE-08) we show that the production of certain OVOCs (e.g. hydroxyacetone) from isoprene photo-oxidation in the lower atmosphere is significantly underpredicted by standard chemistry schemes. A recently suggested novel pathway for isoprene peroxy radicals could explain the observed discrepancy and reconcile the rapid formation of these VOCs. Furthermore, if generalized our observations suggest that prompt photochemical formation of OVOCs and other uncertainties in VOC oxidation schemes could result in substantial underestimates of modelled OH reactivity that could explain a major fraction of the missing OH sink over forests which has previously been attributed to a missing source of primary biogenic VOCs.

1 Introduction

Volatile organic compounds (VOCs) critically influence the composition of the Earth's atmosphere by fueling tropospheric chemistry (Atkinson, 2000), and providing condensable material for organic aerosol formation (Kanakidou et al., 2005). On a global scale the emission strength of biogenic VOCs dominates the annual VOC budget (~1000–2000 Tg/y). A large fraction of this reduced carbon flux enters the atmosphere in form of isoprene, which could exceed global methane emissions (Guenther

ACPD

9, 13629–13653, 2009

et al., 2006). VOCs are emitted from many terrestrial plants at high rates, in particular in tropical ecoregions, and some species are known to re-emit up to 10% of their assimilated carbon in form of isoprene (Kesselmeier et al., 2002). Isoprene is also highly reactive and its photochemical evolution of isoprene therefore plays a central role in atmospheric chemistry. Detailed chemical schemes are needed in global atmospheric chemistry models (e.g. Brasseur et al., 1998; Bey et al., 2001; Kuhlmann et al., 2003) to simulate the tropical photo-reactor and assess how the oxidizing capacity of the remote tropical atmosphere is modulated by this compound. Isoprene chemistry schemes (Fan and Zhang, 2004; Carter and Atkinson, 1996; Pinho et al., 2005) are typically condensed so they can be incorporated in global and regional chemistry models. Most current lumped chemistry schemes include near explicit representation of the first and second generation oxidation products of isoprene (Pfister et al., 2008; Taraborelli et al., 2008; Emmerson and Evans, 2009). Some of these schemes have been applied in field studies conducted in the tropics (e.g. Warneke et al., 2001; Ganzeveld et al., 2008). Recent theoretical and laboratory evidence suggested that some of the basic steps of isoprene peroxy radical cycling are still poorly understood (Dibble, 2002; Paulot et al., 2009; Park et al., 2003). Here we use field measurements of isoprene and its oxidation products methyl vinyl ketone (MVK), methacrolein (MAC) and hydroxyacetone to assess their photochemical evolution at a remote field site approx. 60 km NNW of Manaus in the central Amazon basin during the wet season in 2008.

2 Methods

2.1 Measurement site

Measurements were conducted from 9–28 February 2008 as part of the Amazonian Aerosol Characterization Experiment (AMAZE-08). The site (02° 35.657′ S, 60° 12.557′ W) located in the Reserva Biologica do Cuieiras and managed by the Instituto Nacional de Pesquisas da Amazonia (INPA) and the Large-Scale Biosphere-

ACPD
9, 13629–13653, 2009

Atmosphere Experiment in Amazonia (LBA). The vegetation cover consists of primary tropical rainforest (approx. leaf area index of 5–6 m^2/m^2) with an average canopy height of ~30 m surrounding the ~40 m measurement tower.

2.2 VOC measurement and data analysis

A Proton-Transfer-Reaction Mass Spectrometer was used for gradient measurements of selected VOCs. The instrument is based on soft chemical ionization using protonated water ions (H_3O^+). It combines the advantage of online analysis while maintaining linearity and low detection limits (Ionicon, Austria) (Lindinger et al. 1998; Hansel et al., 1998). The instrument was operated at 2.3 mbar drift pressure and 540 V drift voltage and calibrated using two multicomponent ppmv VOC standards: VOC standard 1 contained a mixture of methanol, acetonitrile, acetaldehyde, acetone, isoprene, methyl vinyl ketone, methyl ethyl ketone, benzene, toluene, m-, o-, p-xylenes and camphene; VOC standard 2 contained a mixture of benzene, toluene, m-, o-, p-xylenes+ethylbenzene, chlorobenzene, trimethylbenzenes, dichlorobenzenes and trichlorobenzenes. Ultrapure hydroxyacetone (SigmaUltra, Sigma Aldrich, CAS 116-09-6, Milwaukee, WI) was injected into the instrument to determine the instrument specific response for this compound. The instrument sequentially sampled of six independent $^1/_4''$ inch Teflon (PFA) sampling lines mounted at 2, 10.9, 16.7, 23.9, 30.3, and 39.8 m on a 40 m tall tower. A valve switching system changed sampling lines every 5 min and cycled through the entire gradient over a 30 min period. Gradients were calculated from the 5 min averages. High flow rates through the sampling lines resulted in delay times of less than 8–12 s, measured by spiking a VOC pulse at each sampling inlet. Isoprene and the sum of MVK and MAC were measured at ion channels *m/z* 69 and *m/z* 71, respectively. Hydroxyacetone was monitored on ion channel *m/z* 75. The detection limits for isoprene, MVK+MAC and hydroxyacetone for a 5 s integration time were 10, 5 and 5 pptv, respectively. Particular sensitivities corresponded to proton-transfer reaction rate constants of 2×10^{-9}, 3×10^{-9} and 3.5×10^{-9} cm^3/s, respectively. PTRMS hydroxyacetone concentration data from earlier field campaigns

(Williams et al., 2001; Holzinger et al., 2007; Stroud et al., 2005) were corrected by the relative difference of the rate constants between hydroxyacetone and isoprene. Potential interferences on *m/z* 75 due to butanol can be excluded as butanol completely dehydrates and is observed exclusively on *m/z* 57 under operating conditions used here. Propionic acid also dehydrates partially into *m/z* 57. Our dataset shows no significant correlation between signals observed on *m/z* 57 and *m/z* 75, which is indicative that propionic acid did not contribute to *m/z* 75. Moreover, the correlation between acetic acid+glycoladehyde observed on *m/z* 61 shows very poor correlation with neither isoprene nor MVK+MAC. The most likely candidate for *m/z* 75 is therefore a compound originating from isoprene oxidation. We can further exclude other interferences such as diethylether and methyl acetate from GC samples. We conclude that the PTRMS mass channel *m/z* 75 was specific for the measurement of hydroxyacetone in this high isoprene environment and confirm conclusions drawn from earlier studies (Williams et al., 2001). GC-MS air samples were collected on carbotrap and tenax cartridges that were stored at approximately 0°C until analysis at NCAR Boulder laboratory, except during transit from Brazil to USA, when they were at ambient temperature for approximately 1 d. The cartridges were desorbed thermally using an NCAR-made system (Greenberg et al., 1994) and analyzed by gas chromatography with mass spectrometric detection (Hapsite Smart, Inficon, East Syracuse NY) using a 30 m×0.32 mm ID 1 mm film DB-1 column, temperature programmed from 40 to 200°C at 3°C per min after an initial 2 min hold. VOC were quantified with respect to NIST traceable standards as described by Greenberg et al. (1994). Ozone (O_3), and nitric oxide (NO) concentrations were also measured via the 6-level sampling manifold. Ozone was measured by UV absorbance (2B Technologies, Model 205) every 10 s and then averaged over the entire 5 min sampling time on each level, excluding only the first 15 s to insure adequate flushing of the connecting gas lines. The ozone analyzer was compared with laboratory instruments both prior to and following the experiment and found to agree with ±5% with a detection limit of 2 ppbv. It was zeroed periodically by placing an ozone scrubber on the 1.5 m inlet. NO was measured by ozone-induced chemiluminescence (Ecophysics, Model

ACPD
9, 13629–13653, 2009

88Y) at a sample rate of 1 s. Measurements were averaged over the first 2 min of sampling on a given level (excluding initial 15 s). During the other 3 min, the air was either passed through a photolytic converter (Droplet Technology, BLC-100) to convert NO_2 to NO or through a molybdenum catalyst which reduces oxidized nitrogen to NO which was subsequently detected by chemiluminescence. The NO analyzer was zeroed automatically every hour by diverting the sample flow through a pre-reactor and adding a large excess of ozone which consumed the NO. It was calibrated periodically during the campaign by standard addition of a known NO concentration to the 2 m inlet. The detection limit was ~ 50 pptv. Laboratory tests indicated no measurable loss of either ozone, NO or NO2 within any of the PFA inlet lines. Wind velocities at 40 m were measured by a 3-dimensional sonic anemometer (Applied Technologies, SATI-K) mounted on a boom extending 2 m from the tower and sampled at 20 Hz.

2.3 VOC gradient fluxes

Ecosystemscale fluxes of VOCs were calculated based on concentration gradients throughout the canopy and applying an Inverse Lagrangian Transport Model (Raupach, 1989; Nemitz et al., 2000; and Karl et al., 2004).

The VOC fluxes were computed according to,

$$\vec{C} - C_{\text{ref}} = \vec{\mathbf{D}} \cdot \vec{S} \quad (1)$$

where $\boldsymbol{C}$ is the VOC concentration ($\mu g/m^3$) vector for each level, C_{ref} is the VOC concentration ($\mu g/m^3$) at reference height (e.g. 30 m), **D** (m) represents a dispersion matrix and $\boldsymbol{S}$ ($mg/m^2/h/m$) the resulting VOC source/sink vector. **D** can be expressed as a function of Lagrangian timescale (Tl) and profiles of the standard deviation of the vertical wind speed (σ_w) divided by the friction velocity (u^*). The calculation was performed using a 10×4 dispersion matrix. Integration over all source and sink terms ($\boldsymbol{S}$) yielded the canopy scale VOC flux ($mg/m^2/h$). Fluxes were calculated for 30 min intervals.

The parameterization of **D** was based on turbulence measurements inside and above

ACPD
9, 13629–13653, 2009

the canopy and calculated using the far- and near-field approach described by Raupach (1989). The Lagrangian timescale was parameterized according to Raupach (1989).

3 Results and discussion

3.1 Vertical canopy profiles

Figure 1a shows the mean integrated vertical source/sink distribution of isoprene, MVK, MAC and hydroxyacetone measured by PTR-MS during daytime (11:00–17:00 LT). The source/sink distribution was inferred from in-canopy concentration measurements using an inverse Lagrangian transport model. The specificity of the PTRMS to monitor isoprene and the sum of MVK+MAC has been demonstrated previously (e.g. de Gouw and Warneke, 2007). Hydroxyacetone was monitored on ion channel *m/z* 75 and was tentatively identified as a major VOC observed by PTRMS in tropical ecosystems in the past (Williams et al., 2001). Average midday ozone mixing ratios (Fig. 1b) were ~8 ppbv decreasing to <3 ppbv near the ground. Isoprene was mostly emitted in the upper part of the canopy as expected because of the light environment and the distribution of sun and shade leaves throughout the canopy. The oxidation products MVK, MAC and hydroxyacetone were deposited to the canopy with maximum deposition occurring near the top. The calculated source/sink distribution integrated over the entire canopy for these VOCs suggests that the primary source was located above the forest.

3.2 Photochemical production of MVK, MAC and hydroxyacetone

The first steps of the photo oxidation of isoprene via the hydroxyl radical (OH) can be summarized as:

$$C_5H_8 + OH \xrightarrow{O2} C_5H_9O_3 \quad (1a)$$

$$C_5H_9O_3 + NO \longrightarrow \text{carbonyls} \quad (1b)$$

ACPD
9, 13629–13653, 2009

$$C_5H_9O_3 + HO_2 \longrightarrow \text{peroxides} \quad (1c)$$

Measured NO mixing ratios were sufficiently high (100–300 pptv, τ~30 s) in the surface layer to dominate over the reaction with HO_2 radical estimates (10–20 pptv; τ~300 s) according to results from a photochemical box model based on the Mozart Chemistry Mechanism v4 (Pfister et al. 2008). Consequently peroxy radical reactions with NO (τ~30 s) led to significant production of the carbonyls methyl vinyl ketone (MVK) and methacrolein (MAC). For measurements reported here Reaction (1a)–(1c) can therefore be simplified to the following kinetic reaction model, where Y is the branching ratio for each channel.

$$\begin{aligned} C_5H_8 + OH &\xrightarrow{Y=0.32} MVK \\ C_5H_8 + OH &\xrightarrow{Y=0.23} MAC \\ MAC + OH &\xrightarrow{Y=0.42} \text{Hydroxyacetone} \\ MVK + OH &\longrightarrow \text{Products} \end{aligned} \quad (2)$$

During daytime the evolution of isoprene chemistry in the planetary boundary layer (PBL) is conceptually different than many environmental chamber experiments in that there is continuous supply of isoprene. As a result the production of compounds originating directly from first generation isoprene peroxy radicals is relatively more prominent in the real atmosphere. For example the ratio of (MVK+MAC)/isoprene will approach infinity in smog chambers, while there is a steady-state upper limit of ~2.4 in the PBL (assuming yields according to Eq. 2 and OH reaction rate constants of 1×10^{-10} cm^3/s, 1.9×10^{-11} cm^3/s and 3.4×10^{-11} cm^3/s for isoprene, MVK and MAC, respectively). However, due to the time-dependent isoprene supply and the slower OH reactions of the products, steady state conditions are rarely reached. During AMAZE-08 a daytime (11:00–17:00 LT) ratio of 0.44 was observed (Fig. 2, black circles). Similar ratios were observed in previous field studies (e.g. Warneke et al., 2001; Kuhn et al., 2007; Eerdekens et al., 2008; Karl et al., 2007). The major source of hydroxyacetone is oxidation of MAC (e.g. Carter and Atkinson, 1996). Figure 2 shows

ACPD
9, 13629–13653, 2009

a correlation plot between hydroxyacetone and the sum of the 1st generation oxidation products MVK and MAC (red circles). For a given MVK+MAC to isoprene ratio of 0.44 we calculate a slope of 0.03 between hydroxyacetone and MVK+MAC according to Eq. 2 (assuming constant isoprene emissions). This is ∼10 times smaller than the observed ratio (0.31) and implies that an additional source of hydroxyacetone, which is highly correlated with the oxidation products MVK and MAC (R^2=0.79) and isoprene (R^2=0.70), is missing. The high degree of correlation suggests that the missing source of hydroxyacetone comes from within the isoprene oxidation chain, but has to be faster than the production from MAC, which is thought to be the major contributor to the secondary formation of hydroxyacetone. Other possible chemical sources of hydroxyacetone include oxidation of peroxides originating from propene and production from acetone oxidation (e.g. acetonyl peroxy radicals reacting with methyl peroxy radicals). However, both of these are expected to be slow due to the low concentrations of propene and subsequent peroxides or the need for radical-radical reactions in the case of acetone oxidation. Since isoprene mixing ratios (e.g. up to 8 ppbv) dominate the tropical environment these processes must compete with the dominant production path via MAC. Although anticipated to be small in the wet season of the central Amazon Basin, another possible source of hydroxyacetone is biomass burning. We investigated this using acetonitrile as specific gas phase marker. Periods of elevated acetonitrile (∼10% of the entire dataset) were excluded from the analysis, however the contribution from biomass burning was likely small even during periods of elevated acetonitrile. As an example a maximum acetonitrile mixing ratio enhancement of 0.6 ppbv was observed. Based on a previous study (Karl et al., 2007) this could lead to a mixing ratio increase of ∼0.18 ppbv for hydroxyacetone, roughly 10% of the maximum values observed during this study (Fig. 2). A further argument against a significant biomass burning source is the good correlation observed between hydroxyacetone and MVK+MAC as well as with isoprene. In order to check whether the observed ratios between isoprene, MVK+MAC and hydroxyacetone are comparable to previous datasets we have re-analyzed data reported in the literature. The triangular plot shown in Fig. 3a summarizes findings

ACPD
9, 13629–13653, 2009

from 5 field campaigns, including the present study, conducted near isoprene emission sources (Williams et al., 2001; Holzinger et al., 2007; Stroud et al., 2005; Spaulding et al., 2003). Concentrations from these datasets, which are representative for typical local noontime conditions, were normalized by the sum of isoprene, MVK, MAC and hydroxyacetone in order to quantitatively compare their relative ratios. The colour coded triangular symbols represent a trajectory along which the relative ratios would evolve according to Eq. (2). The colour coding indicates photochemical age (time exposure to OH). Due to a constant supply of isoprene the theoretical trajectory ends at the steady state limit, typically reached after 10^7 molecules cm^{-3} days of OH exposure for the reaction sequence discussed here. Measured distributions from all field observations, in particular the AMAZE dataset discussed here, show that hydroxyacetone mixing ratios are significantly higher than what would be expected from the reaction model described by Eq. (2) when only production from MAC is assumed. The discrepancy becomes larger for data collected closer to the source (recent supply of isoprene). The only way to reconcile such fast production of hydroxyacetone is to include a direct production path from isoprene (e.g. through isoprene alkenoxy radicals). We extended the set of reactions listed in Eq. (2) by including direct production from isoprene plus OH and obtained an optimal yield (Y_{iso}) based on a non-linear least square regression procedure of the coupled set of differential equations (Eq. 2). The black line in Fig. 3b shows the case where no direct production of hydroxyacetone is assumed (Y_{iso}=0). The blue line in Fig. 3b depicts a curve based on direct production with a fitted Y_{iso} of 8.3 (±2.2)%, which would be sufficient to explain the observed distribution of hydroxyacetone in isoprene dominated environments. For reference the same curve is also shown by the colour coded circles depicted in Fig. 3a. Dibble (2002) recently conducted a theoretical study on the decomposition of certain isoprene–alkenoxy radicals and hypothesized a direct channel which would lead to the formation of products typically associated with secondary and tertiary chemistry (e.g. hydroxyacetone and glyoxal). Preliminary constraints from environmental chamber experiments have tentatively invoked a similar mechanism to explain the formation of organic acids and organic nitrates under high

ACPD
9, 13629–13653, 2009

NO_x environments (Paulot et al., 2009). These independent studies support our field observations, which suggest that the production of hydroxyacetone from isoprene oxidation is larger than assumed by current chemistry schemes. The effect of this rapid formation becomes particularly apparent in the tropical PBL, where a continuous supply of isoprene from the vegetation fuels the production of oxygenated VOCs (OVOC).

3.3 OH reactivity

If generalized our findings have implications for OH reactivity measurements (di Carlo et al., 2004; Sinha et al., 2008) conducted close to isoprene emission sources. OH is considered the main oxidant in the atmosphere and reacts with all VOCs. The reaction frequency of a VOC with OH is defined as the product of its rate-coefficient times its concentration. The sum of all reaction frequencies is the inverse of the OH lifetime and is termed OH reactivity. The measurement of OH reactivity has been used as a top-down constraint to infer VOC sources in the atmosphere (e.g. di Carlo et al., 2004; Sinha et al., 2008). However, since all reactive VOCs are not always measured concurrently, photochemical models must be used to estimate contributions of many species to the overall OH reactivity. Rapid formation of isoprene oxidation products could lead to a higher modelled OH reactivity than assumed based on current photo-oxidation mechanisms. This becomes particularly important when lumped chemical schemes are used (di Carlo et al., 2004), which further simplify the chemical degradation mechanism of VOCs. In order to test the impact of our observations on modelled OH reactivity, we have incorporated an extensive set of reactions (appendix) in a kinetic reaction model and calculated the evolution of the OH reactivity of isoprene oxidation products assuming fast production of OVOCs and constant supply of isoprene (Fig. 4). For typical conditions and datasets discussed here the OH reactivity from photo-oxidation products for the standard run (no fast OVOC production) could account for 20–150% of the measured reactivity relative to isoprene depending on the photochemical age. Formaldehyde, an important intermediate isoprene oxidation product, accounts for 30% of the OVOC reactivity based on the photo-oxidation

scheme used here which includes the eleven most prominent OVOCs produced within the isoprene oxidation chain (Table 1). Together the major oxidation products MVK, MAC and HCHO account for 75% of the OVOC reactivity. Adding rapid formation of OVOCs to this scheme could increase the reactivity of photo-oxidation products relative to isoprene by up to 20% (e.g. gray line, Fig. 4). Figure 4 also shows the evolution of isoprene photo-oxidation products based on the Regional Atmospheric Chemistry Mechanism (RACM) (excluding the contribution from terminal alkenes OLT) (Stockwell et al., 1997), which has previously been used to model OH reactivity for studies of missing OH sinks (di Carlo et al., 2004). For comparison we also show the evolution of OVOCs derived from isoprene oxidation calculated using the Mozart Chem (v4) mechanism used for global modelling studies (Pfister et al., 2008). The RACM mechanism predicts an OH reactivity that could be as much as ~40–50% lower than the combined OH reactivity calculated here that is independent of photochemical age. Based on the presented evidence we conclude that a large fraction of the missing VOCs inferred from OH reactivity measurements in forested environments (e.g. >50–70%) could be an overestimate associated with isoprene oxidation products not accounted for by lumped photo-chemical oxidation schemes. Given the fact that many OVOCs were typically not measured during previously reported discrepancies between modelled and measured OH reactivity (di Carlo et al., 2004; Mao et al., 2009) the actual missing OH sink could be much smaller and perhaps reconciled without the need to invoke large missing sources of unknown primary biogenic VOCs.

4 Conclusion and summary

While focusing on a subset of OVOCs produced during the photochemical degradation of isoprene, our field observations in the wet season of the central Amazon Basin show that the production of certain OVOCs is higher than current chemical photo-oxidation mechanisms can explain. Our measurements demonstrate the importance of accurate representation of OVOCs, which act as an OH sink and precursors for secondary

ACPD
9, 13629–13653, 2009

organic aerosols (SOA). To date only a few studies (Spaulding et al., 2003; Warneke et al., 2001) have reported field measurements of selected OVOCs produced from isoprene chemistry. A more extensive set of OVOC observations will be necessary to fully constrain OH reactivity measurements in the future and will help improve uncertainties associated with modelling OH lifetimes in isoprene dominated environments. We conclude that a better understanding of the photo-chemical evolution of OVOCs is absolutely critical to improve uncertainties in oxidant and organic carbon budgets in the troposphere.

Appendix A

A sequential reaction model was used to calculate the evolution of prominent isoprene photo oxidation products. Table 1 lists compounds included in the present analysis. Due to poor understanding of atmospheric oxidation of some OVOCs the sequential reaction model was restricted to first, second and third generation products exhibiting OH reaction rate coefficients greater than 1×10^{-12} cm^3/s. The selection was also based on the fact that the present analysis is restricted to photochemical ages of $<2\times10^6$ molecules/cm^3 d, typically encountered close to isoprene emission sources. In addition the evolution of OVOCs was calculated using two lumped chemistry schemes (Mozart Chem version 4, Pfister et al., 2008; and RACM, Stockwell et al., 1997). The Mozart Chemistry scheme is used in a global atmospheric chemistry model and includes nearly explicit representation of the 1st and 2nd generation oxidation products from isoprene. The Regional Atmospheric Chemistry Mechanism (RACM) was originally developed for regional air quality purposes and exhibits a higher degree of lumping for isoprene products than the Mozart Chemistry scheme.

Acknowledgements. The authors thank the entire AMAZE team for their excellent support and vital collaboration. The National Center for Atmospheric Research is operated by the University Corporation for Atmospheric Research under sponsorship from the National Science Foundation.

References

Atkinson, R.: Atmospheric chemistry of VOCs and NOx, Atmos. Environ., 34, 2063–2101, 2000.

Atkinson, R., Baulch, D. L., Cox, R. A., Hampson, R. F., Jr., Kerr, J. A., Rossi, M. J., and Troe, J.: Evaluated kinetic, photochemical and heterogeneous data for atmospheric chemistry: supplement V, IUPAC subcommittee on gas kinetic data evaluation for atmospheric chemistry, J. Phys. Chem. Ref. Data, 26, 521–1011, 1997.

Bacher, C., Tyndall, G. S., and Orlando, J. J.: The atmospheric chemistry of glycolaldehyde, J. Atmos. Chem., 39(2), 171–189, 2001.

Bey I., Jacob, D. J., Yantosca, R. M., Logan, J. A., Field, B., Fiore, A. M., Li, Q., Liu, H., Mickley, L. J., and Schultz, M.: Global modeling of tropospheric chemistry with assimilated meteorology: model description and evaluation, J. Geophys. Res., 106, 23073–23096, 2001.

Brasseur, G. P., Hauglustaine, D. A., Walters, S., Rasch, P. J., Muller, J.-F., Granier, C., and Tie, X.-X.: MOZART. A global chemical transport model for ozone and related chemical tracers, Part 1: Model description, J. Geophys. Res., 103, 28265–28289, 1998.

Carter, W. P. L. and Atkinson, R.: Development and evaluation of a detailed mechanism for atmospheric reactions of isoprene and NO_x, Int. J. Chem. Kinetics, 28, 497–530, 1996.

Carlo, P. D., Brune, W. H., Martinez, M., Harder, H., Lesher, R., Ren, X., Thornberry, T., Carroll, M. A., Young, V., Shepson, P. B., Riemer, D., Apel, E., and Campbell, C.: Missing OH reactivity in a forest: evidence for unkown reactive biogenic VOCs, Science, 304, 722–725, 2004.

Claeys, M., Graham, B., Vas, G., Wang, W., Vermeylen, R., Pashynska, V., Cafmeyer, J., Guyon, P., Andreae, M. O., Artaxo, P., and Maenhaut, W.: Formation of secondary organic aerosols through photooxidation of isoprene, Science, 303, 1173–1176, 2004.

Dibble, T.: Isomerisation of OH-isoprene adducts and hydroxyalkoxy isoprene radicals, J. Phys. Chem. A, 106, 6643–6650, 2002.

Dillon, T. J., Horowitz, A., Holscher, D., Crowley, J. N., Vereecken, L., and Peeters, J.: Reaction of HO with hydroxyacetone ($HOCH_2C(O)CH_3$): rate coefficients (233–363 K) and mechanism, Phys. Chem. Chem. Phys, 8, 236–246, 2006.

de Gouw, J. and Warneke, C.: Measurements of volatile organic compounds in the earths atmosphere using proton-transfer-reaction mass spectrometry, Mass Spectrom. Rev., 26, 223–257, 2007.

Emmerson, K. M. and Evans, M. J.: Comparison of tropospheric gas-phase chemistry schemes for use within global models, Atmos. Chem. Phys., 9, 1831–1845, 2009, http://www.atmos-chem-phys.net/9/1831/2009/.

Eerdekens, G., Ganzeveld, L., Vilà-Guerau de Arellano, J., Klüpfel, T., Sinha, V., Yassaa, N., Williams, J., Harder, H., Kubistin, D., Martinez, M., and Lelieveld, J.: Flux estimates of isoprene, methanol and acetone from airborne PTR-MS measurements over the tropical rainforest during the GABRIEL 2005 campaign, Atmos. Chem. Phys. Discuss., 8, 12903–12969, 2008, http://www.atmos-chem-phys-discuss.net/8/12903/2008/.

Fan, J. and Zhang, R.: Atmospheric oxidation mechanism of isoprene, Environ. Chem., 1, 140–149, 2004.

Ganzeveld, L., Eerdekens, G., Feig, G., Fischer, H., Harder, H., Knigstedt, R., Kubistin, D., Martinez, M., Meixner, F. X., Scheeren, H. A., Sinha, V., Taraborrelli, D., Williams, J., Vilà-Guerau de Arellano, J., and Lelieveld, J.: Surface and boundary layer exchanges of volatile organic compounds, nitrogen oxides and ozone during the GABRIEL campaign, Atmos. Chem. Phys., 8, 6223–6243, 2008, http://www.atmos-chem-phys.net/8/6223/2008/.

Greenberg, J. P. and P. R. Zimmerman: Nonmethane hydrocarbons in remote tropical, continental, and marine atmospheres, J. Geophys. Res., 89(ND3), 4767–4778, 1984.

Gierczak, T., Burkholder, J. B., Talukdar, R. K., Mellouki, A., Barone, S. B., and Ravishankara, A. R.: Atmospheric fate of methyl vinyl ketone and methacrolein, J. Photoch. Photobio. A, 110, 1–10, 1997.

Greenberg, J. P. and Zimmerman, P. R.: Nonmethane hydrocarbons in remote tropical, continental, and marine atmospheres, J. Geophys. Res., 89, 4767–4778, 1984.

Greenberg, J., Lee, B., Helmig, D., and Zimmerman, P.: Fully automated gas chromatograph-flame ionization detector system for the in situ determination of atmospheric non-methane hydrocarbons at low parts per trillion concentration, J. Chromatogr., 676, 389–398, 1994.

Guenther, A., Karl, T., Harley, P., Wiedinmyer, C., Palmer, P. I., and Geron, C.: Estimates of global terrestrial isoprene emissions using MEGAN (Model of Emissions of Gases and Aerosols from Nature), Atmos. Chem. Phys., 6, 3181–3210, 2006, http://www.atmos-chem-phys.net/6/3181/2006/.

Hansel, A., Jordan, A., Warneke, C., Holzinger, R., and Lindinger, W.: Improved detection limit of the proton-transfer reaction mass spectrometer: on-line monitoring of volatile organic

ACPD

9, 13629–13653, 2009

compounds at mixing ratios of a few pptv, Rapid Commun. Mass Sp., 12, 871–875, 1998.
Holzinger, R., Millet, D. B., Williams, B., Lee, A., Kreisberg, N., Hering, S. V., Jimenez, J., Allan, J. D., Worsnop, D. R., and Goldstein, A. H.: Emission, oxidation, and secondary organic aerosol formation of volatile organic compounds as observed at Chebogue Point, Nova Scotia, J. Geophys. Res., 112, D10S24, doi:10.1029/2006JD007599, 2007.
Kanakidou, M., Seinfeld, J. H., Pandis, S. N., Barnes, I., Dentener, F. J., Facchini, M. C., Van Dingenen, R., Ervens, B., Nenes, A., Nielsen, C. J., Swietlicki, E., Putaud, J. P., Balkanski, Y., Fuzzi, S., Horth, J., Moortgat, G. K., Winterhalter, R., Myhre, C. E. L., Tsigaridis, K., Vignati, E., Stephanou, E. G., and Wilson, J.: Organic aerosol and global climate modelling: a review, Atmos. Chem. Phys., 5, 1053–1123, 2005, http://www.atmos-chem-phys.net/5/1053/2005/.
Karl, T., Potosnak, M., Guenther, A., Clark, D., Walker, J., Herrick, J. D., and Geron, C.: Exchange processes of volatile organic compounds above a tropical rain forest: implications for modeling tropospheric chemistry above dense vegetation, J. Geophys. Res., 109, D18306, doi:10.1029/2004JD004738, 2004.
Karl, T., Guenther, A., Yokelson, R. J., Greenberg, J., Potosnak, M., Blake, D. R., and Artaxo, P.: The tropical forest and fire emissions experiment: emission, chemistry, and transport of biogenic volatile organic compounds in the lower atmosphere over Amazonia, J. Geophys. Res., 112, D18302, doi:10.1029/2007JD008539, 2007.
Karl, T. G., Christian, T. J., Yokelson, R. J., Artaxo, P., Hao, W. M., and Guenther, A.: The Tropical Forest and Fire Emissions Experiment: method evaluation of volatile organic compound emissions measured by PTR-MS, FTIR, and GC from tropical biomass burning, Atmos. Chem. Phys., 7, 5883–5897, 2007, http://www.atmos-chem-phys.net/7/5883/2007/.
Kesselmeier, J., Ciccioli, P., Kuhn, U., Stefani, P., Biesenthal, T., Rottenberger, S., Wolf, A., Vitullo, M., Valentini, R., Nobre, A., Kabat, P., and Andreae, M. O.: Volatile organic compound emissions in relation to plant carbon fixation and the terrestrial carbon budget, Global Biogeochem. Cy., 16, 1126, doi:10.1029/2001GB001813, 2002.
Kroll, J. H., Ng, N. L., Murphy, S. M., Flagan, R. C., and Seinfeld, J. H.: Secondary organic aerosol formation from isoprene photooxidation, Environ. Sci. Technol., 40, 1869–1877 2006.
von Kuhlmann, R., Lawrence, M. G., Pschl, U., and Crutzen, P. J.: Sensitivities in global scale modeling of isoprene, Atmos. Chem. Phys., 4, 1–17, 2004,

http://www.atmos-chem-phys.net/4/1/2004/.
Kuhn, U., Andreae, M. O., Ammann, C., Araújo, A. C., Brancaleoni, E., Ciccioli, P., Dindorf, T., Frattoni, M., Gatti, L. V., Ganzeveld, L., Kruijt, B., Lelieveld, J., Lloyd, J., Meixner, F. X., Nobre, A. D., Pöschl, U., Spirig, C., Stefani, P., Thielmann, A., Valentini, R., and Kesselmeier, J.: Isoprene and monoterpene fluxes from Central Amazonian rainforest inferred from tower-based and airborne measurements, and implications on the atmospheric chemistry and the local carbon budget, Atmos. Chem. Phys., 7, 2855–2879, 2007, http://www.atmos-chem-phys.net/7/2855/2007/.
Kwok, E. S.C., Aschmann, S. M., and Atkinson, R.: Rate constants for the gas-phase reaction of selected carbamates and lactates, Environ. Sci. Technol., 30, 329–34, 1996.
Lindinger, W., Jordan, A., and Hansel, A.: Proton-transfer-reaction mass spectroscopy (PTR-MS): on-line monitoring of volatile organic compounds at pptv levels, Chem. Soc. Rev., 27, 347–534, 1998.
Nemitz, E., Sutton, M. A., Gut, A., Jose, R. S., Husted, S., and Schjoerring, J. K.: Sources and sinks of ammonia within an oilseed rape canopy, Agr. Forest Meteorol., 105, 385–404, 2000.
Park, J., Candice, G. J., Zhang, R., and North, S. W.: Cyclization reactions in isoprene derived β-hydroxy radicals: implications for the atmospheric oxidation mechanism, Phys. Chem. Chem. Phys., 5, 3638–3642, 2003.
Paulot, F., Crounse, J. D., Kjaergaard, H. G., Kroll, J. H., Seinfeld, J. H., and Wennberg, P. O.: Isoprene photooxidation: new insights into the production of acids and organic nitrates, Atmos. Chem. Phys., 9, 1479–1501, 2009, http://www.atmos-chem-phys.net/9/1479/2009/.
Pfister, G. G., Emmons, L. K., Hess, P. G., Lamarque, J. F., Orlando, J. J., Walters, S., Guenther, A., Palmer, P. I., and Lawrence, P. J.: Contribution of isoprene to chemical budgets: a model tracer study with the NCAR CTM MOZART-4, J. Geophys. Res., 113, D05308, doi:10.1029/2007JD008948, 2008.
Pinho, P. G., Pio, C. A., and Jenkin, M. E.: Evaluation of isoprene degradation in the detailed tropospheric chemical mechanism, MCM v3, using environmental chamber data, Atmos. Environ., 39, 1303–1322, 2005.
Raupach, M. R.: A practical Lagrangian method for relating scalar concentrations to source distributions in vegetation canopies, Quart. J. Roy. Meteor. Soc., 115, 609–632, 1989.
Sinha, V., Williams, J., Crowley, J. N., and Lelieveld, J.: The Comparative Reactivity Method a new tool to measure total OH Reactivity in ambient air, Atmos. Chem. Phys., 8, 2213–2227,

2008,
http://www.atmos-chem-phys.net/8/2213/2008/.
Spaulding, R. S., Schade, G. W., Goldstein, A. H., and Charles, M. J.: Characterization of secondary atmospheric photooxidation products: evidence for biogenic and anthropogenic sources, J. Geophys. Res., 108, D84247, doi:10.1029/2002JD002478, 2003.
Stockwell, W. R., Kirchner, F., Kuhn, M., and Seefeld, S.: A new mechanism for regional atmospheric chemistry modeling, J. Geophys. Res., 102, 25847–25879, 1997.
Stroud, C., Makar, P., Karl, T., Guenther, A., Geron, C., Turnipseed, A., Nemitz, E., Baker, B., Potosnak, M., and Fuentes, J. D.: Role of canopy-scale photochemistry in modifying biogenic-atmosphere exchange of reactive terpene species: results from the CELTIC field study, J. Geophys. Res., 110, D17303, doi:10.1029/2005JD005775, 2005.
Taraborrelli, D., Lawrence, M. G., Butler, T. M., Sander, R., and Lelieveld, J.: Mainz Isoprene Mechanism 2 (MIM2): an isoprene oxidation mechanism for regional and global atmospheric modelling, Atmos. Chem. Phys., 9, 2751–2777, 2009,
http://www.atmos-chem-phys.net/9/2751/2009/.
Warneke, C., Holzinger, R., Hansel, A., Jordan, A., Lindinger, W., Poeschl, U., Williams, J., Hoor, P., Fischer, H., Crutzen, P. J., Scheeren, H. A., and Lelieveld, J.: Isoprene and its oxidation products methyl vinyl ketone, methacrolein, and isoprene related peroxides measured online over the 5 tropical rain forest of Surinam in March 1998, J. Atmos. Chem., 38, 167–185, 2001.
Williams, J., Poeschl, U., Crutzen, P. J., Hansel, A., Holzinger, R., Warneke, C., Lindinger, W., and Lelieveld, J.: An atmospheric chemistry interpretation of mass scans obtained from a proton transfer mass spectrometer flown over the tropical rainforest of Surinam, J. Atmos. Chem., 38, 133–166, 2001.

Table 1. VOCs considered for the sequential reaction model.

VOC	Rate Coefficient (295K) (cm^3/s)	Photolysis[(g)] (1/s)
Isoprene (C_5H_8)	1.0×10^{10}[(a),(b)]	–
Methylvinylketone (MVK)	1.9×10^{11}[(a),(b)]	1.2×10^{6}
Methacrolein (MAC)	3.4×10^{11}[(a),(b)]	2.2×10^{6}
Hydroxyacetone (HYAC)	6.0×10^{12}[(c)]	$<1\times10^{6}$
Glycolaldehyde (GLYALD)	1.1×10^{11}[(d)]	4×10^{6}
Methylglyoxal (MeGLYO)	1.7×10^{11}[(a)]	1×10^{4}
Glyoxal (GLYO)	1.2×10^{11}[(a)]	6×10^{5}
Formaldehyde (HCHO)	1.0×10^{11}[(a)]	4×10^{5}[(h)]
3-Methylfuran (MF)	9.3×10^{11}[(a)]	–
$C_5H_8O_2$ (e.g. 4-Hydroxy-2-methylbut-2enal) (HC5)	5.0×10^{11}[(e)]	$<1\times10^{6}$
Methylethylketone (MEK)	1.3×10^{12}[(f)]	7×10^{7}
Acetaldehyde (CH_3CHO)	1.4×10^{11}[(f)]	5×10^{6}

[(a)] Carter and Atkinson (1996)
[(b)] Gieczak et al. (1997)
[(c)] Dillon et al. (2006)
[(d)] Bacher et al. (2001)
[(e)] Estimated based on Kwok et al. (1996)
[(f)] Atkinson et al. (1997)
[(g)] From Tropospheric Ultraviolet and Visible (TUV) Radiation Model: http://cprm.acd.ucar.edu/Models/TUV/
[(h)] For molecular and radical branch

ACPD
9, 13629–13653, 2009

Table 2. Simplified sequential reaction model used to calculate OH reactivity based on VOCs listed in Table 1. Production of CO is not included.

Reaction: VOC+OH	Products
Isoprene (C_5H_8)	0.63 HCHO + 0.32 MVK + 0.23 MAC + Y_{iso} HYAC + Y_{iso} GLYALD + Y_{iso} MeGLYO + Y_{iso} GLYO + Y_{iso} MF + 0.1 HC5[(1)]
Methylvinylketone (MVK)	0.65 GLYALD + 0.3 MeGLYO + 0.3 HCHO
Methacrolein (MAC)	0.42 HYAC + 0.08 MeGLYO + 0.50 HCHO
Hydroxyacetone (HYAC)	0.91 MeGLYO + (0.125 Acetic Acid)[(2)]
Glycolaldehyde (GLYALD)	0.2 GLYO + 0.8 HCHO
$C_5H_8O_2$ (e.g. 4-Hydroxy-2-methylbut-2enal) (HC5)	0.5 MEK + 0.25 GLYALD + 0.25 MeGLYO
Methylethylketone	CH_3CHO

[(1)] Y_{iso}=(0.083±0.022): Yield based on estimated yields for hydroxyacetone

[(2)] Further photooxidation of acetic acid is neglected due to slow reaction rate

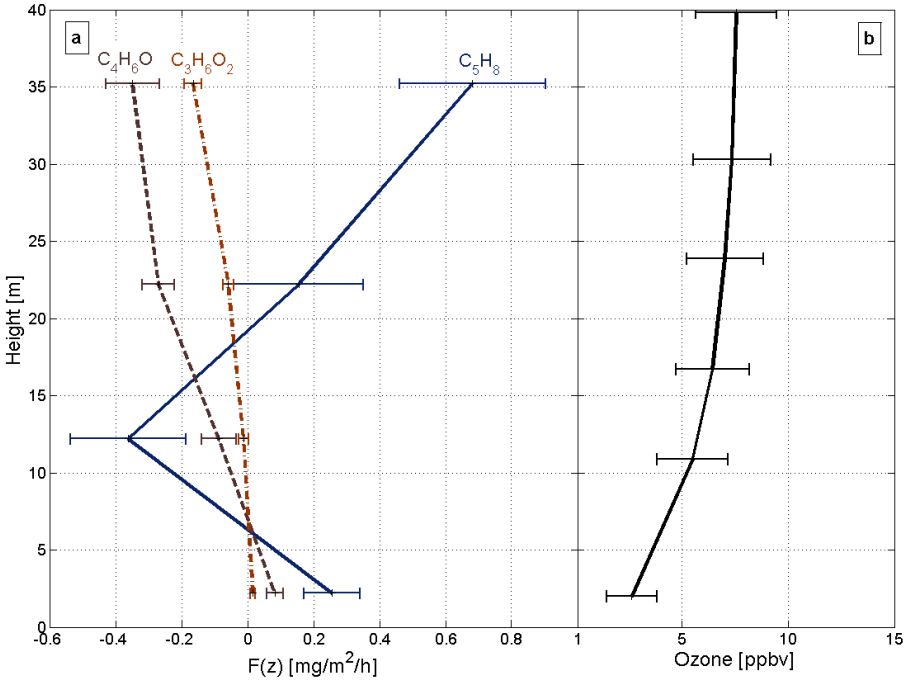

Fig. 1. Integrated flux and concentration profiles through 30 m canopy. **(a)** Integrated flux profiles of Isoprene (C_5H_8), MVK+MAC (C_4H_6O) and Hydroxyacetone ($C_3H_6O_2$). **(b)** Ozone concentration profile.

ACPD
9, 13629–13653, 2009

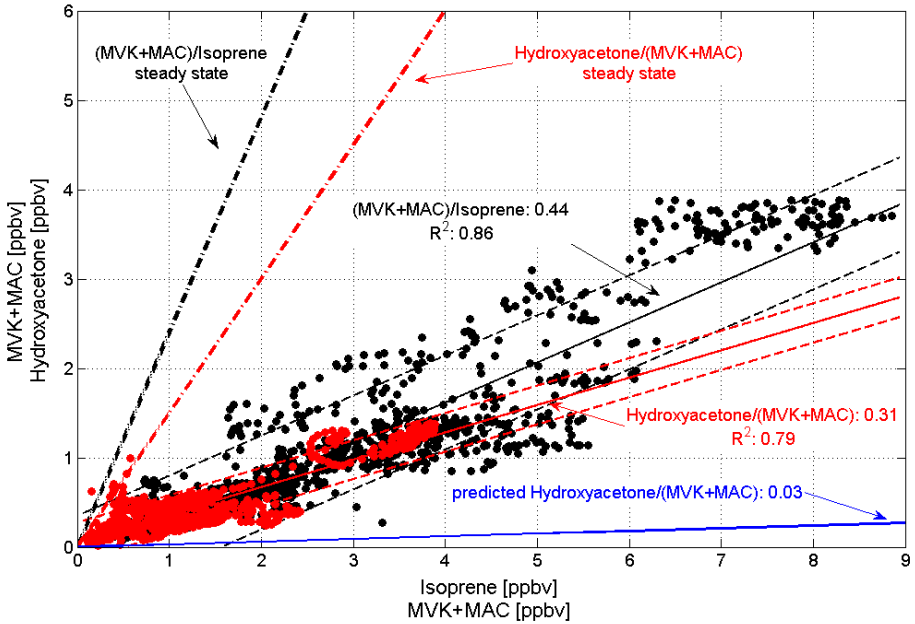

Fig. 2. Correlation between MVK+MAC and isoprene and between hydroxyacetone and MVK+MAC. Regressions based on a robust fitting procedure are indicated by solid black and red lines. Thin dashed lines indicate 85% prediction interval for regressions. Modelled hydroxyacetone/(MVK+MAC) slope is depicted by the blue solid line. Also shown are steady state limits (dashed dotted lines).

ACPD
9, 13629–13653, 2009

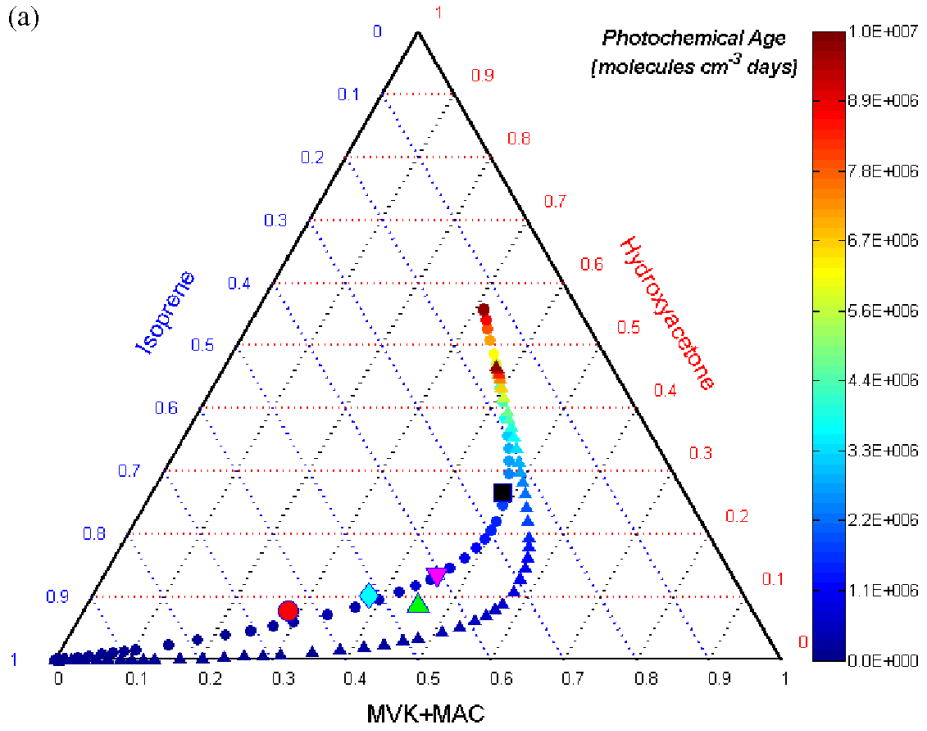

Fig. 3a. Triangular correlation plot between Isoprene, MVK+MAC and hydroxyacetone mixing ratios normalized to 1. Modelled concentrations are colour coded by photochemical age. Triangles represent the standard scheme (no fast production). Circles show case that includes fast production based on the regression shown in Fig. 3b. Field datasets are depicted by symbols as following: red circle (AMAZE, 2008)[this study], blue diamond (LBA-Claire, 1999; Williams et al., 2001), green triangle (CELTIC 2003; Stroud et al. 2005), magenta triangle (ICARTT, 2004; Holzinger et al., 2007) and black square (Blodgett Forest, 2003; Spaulding et al., 2003). Booth trajectories end at the steady state limit, typically reached after 10^7 molecules cm^{-3} d of OH exposure.

ACPD
9, 13629–13653, 2009

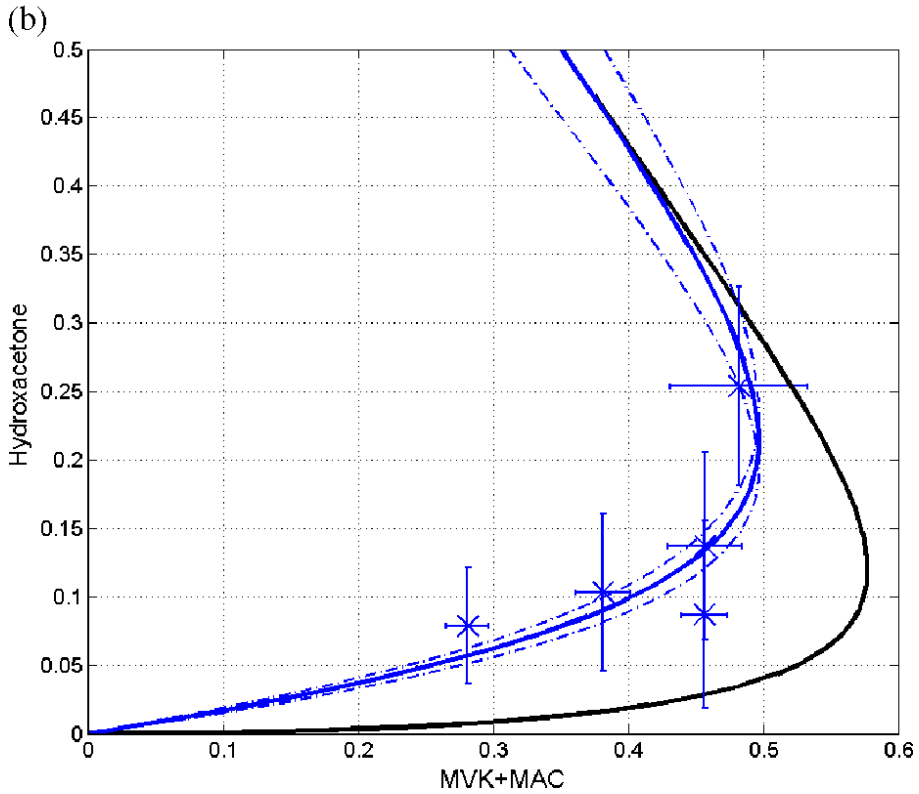

Fig. 3b. Non linear regression to infer the yield for the direct production of hydroxylacetone from isoprene (Y_{iso}) (blue line). Data points represent 5 different studies (see Fig. 3a). Black line depicts standard case with no production from isoprene (Y_{iso}=0). Dashed blue lines indicate 95% confidence interval.

ACPD
9, 13629–13653, 2009

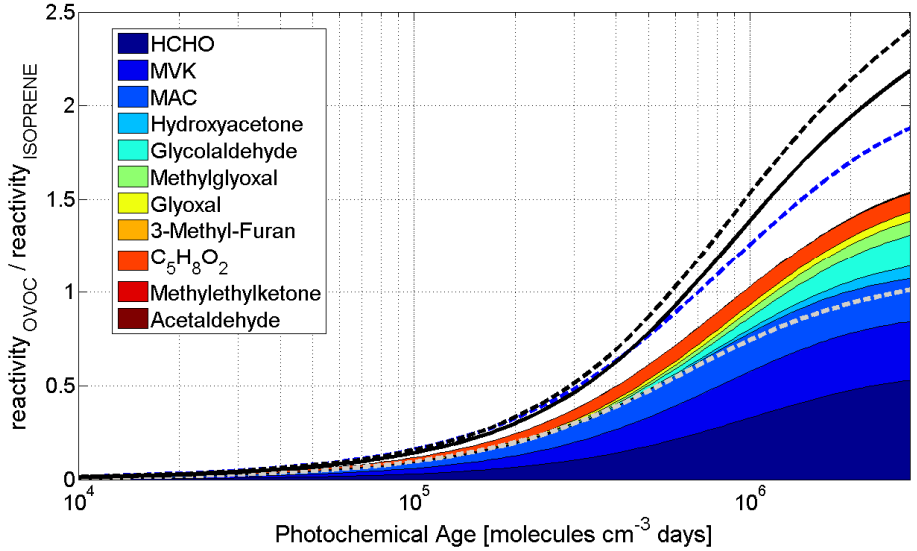

Fig. 4. Evolution of OH reactivity of oxidation products relative to isoprene as a function of photochemical age calculated using a kinetic reaction model. Blue dashed line: including fast production of OVOCs according to Table 2. Also plotted are results from two lumped chemical mechanisms: Black line: Mozart Chemistry (v4), black dashed line: Mozart Chemistry (v4) including fast production of OVOCs, dashed gray line: RACM mechanism.

ACPD
9, 13629–13653, 2009